J Mater Sci (2006) 41:7466–7473
DOI 10.1007/s10853-006-0791-3

Effect of chopped Si–Al–C fiber addition on the mechanical properties of silicon carbide composite

Masanori Sato · Kiyoshi Itatani · Tsuyoshi Tanaka · Ian J. Davies · Seiichiro Koda

Received: 12 February 2005 / Accepted: 29 November 2005 / Published online: 20 September 2006

Abstract Silicon carbide (SiC) composites containing 0–50 mass% of chopped Tyranno® Si–Al–C (SA) fiber (mean length: 214 μm (SA(214)), 394 μm (SA(394)), and 706 μm (SA(706)) were fabricated using the hot-pressing technique at 1800 °C for 30 min under a uniaxial pressure of 31 MPa in Ar atmosphere. The maximum flexural strength of the SiC composite was 344 MPa for 30 mass% of SA(706) fiber addition, whilst the maximum fracture toughness was 4.7 MPa $m^{1/2}$ for 40 mass% of SA(706) fiber addition. Increasing the mean fiber length from 214 to 706 μm decreased the flexural strength from 380 to 281 MPa for 30 mass% of fiber addition, whilst the fracture toughness increased from 3.4 to 4.7 MPa $m^{1/2}$ for 40 mass% of fiber addition. Through use of a treated SA(706) fiber containing an approximately 100 nm surface layer of carbon, the fracture toughness further increased to 6.0 MPa $m^{1/2}$ for 40 mass% of fiber addition; this value was more than twice that of the monolithic SiC ceramic and is believed to be the highest so far achieved for this type of SiC/SiC composite containing chopped fibers.

M. Sato · K. Itatani (✉) · T. Tanaka · S. Koda
Department of Chemistry, Faculty of Science and Engineering, Sophia University, 7-1 Kioi-cho, Chiyoda-ku, Tokyo 102-8554, Japan
e-mail: itatani@sophia.ac.jp

I. J. Davies
Department of Mechanical Engineering, Curtin University of Technology, GPO Box U1987, Perth, WA 6845, Australia

Introduction

Silicon carbide (SiC) ceramics are known to possess excellent corrosion and oxidation resistance and, therefore, various potential applications exist which make use of these properties at elevated temperature, e.g., structural and aerospace development materials, and semiconductor devices [1]. However, the relatively low fracture toughness of monolithic SiC ceramic [2] has resulted in significant attention being paid to the fabrication of ceramic matrix composites (CMCs) containing continuous fibers within a SiC matrix [3], that would be expected to result in increased fracture toughness. For example, the fracture toughness of SiC ceramic reinforced with continuous Tyranno® Si–Ti–C–O fibers has attained 40 MPa $m^{1/2}$ [4]. In addition, ceramic fibers often possess a relatively high strain to failure (typically > 0.5% [5]), compared to that of the SiC matrix. When these ceramic fibers are used in conjunction with a suitable fiber/matrix interface, the failure of the composite was shown to be ''pseudo-ductile'', due to crack deflection and debonding at the fiber/matrix interface, followed by fiber pull-out [6–8].

Much work has, therefore, been carried out on continuous fiber-reinforced CMCs. In contrast to this, relatively little attention has been paid to the reinforcement of CMCs by discontinuous fibers [9–13], mainly due to their low fracture toughness compared to that of continuous fiber-reinforced composites. Nevertheless, there are other advantages, such as precise control of the fiber amount, reduced fabrication costs, and simpler production of complex shapes. The present authors have fabricated and evaluated the mechanical properties of hot-pressed SiC ceramics containing chopped Tyranno® Si–Zr–C–O (SZ) fibers

(mean length: ≈ 0.5 mm) and noted an increase in fracture toughness of 40% compared to the monolithic case [10]. The recent development of crystalline near-stoichiometric Tyranno® Si–Al–C (SA) fiber [14] has further increased the potential operating temperature range of SiC/SiC composites, due to the excellent heat resistance of these fibers, e.g., >2.5 GPa tensile strength between room temperature and 1900 °C in an inert atmosphere [14]. Lee and Yano [13] have investigated the properties of SiC/SiC composites containing chopped SA fiber (mean length: ≈ 1 mm) with a maximum three-point bend strength of 260 MPa being achieved at room temperature. The present authors have recently conducted a preliminary investigation of the fracture toughness of hot-pressed SiC/SiC composites containing chopped SA fibers (mean length: 394 μm) with a maximum value of 5.8 MPa $m^{1/2}$ being achieved [15]. In the present work the authors have extended their previous investigation and examined the effect of mean fiber length and fiber amount on the mechanical properties (flexural strength and fracture toughness) of high density hot-pressed SiC/SiC composites reinforced with chopped SA fiber.

Experimental procedure

Preparation of the powder and compacts

The starting SiC and sintering aid (aluminum carbide (Al_4C_3)) powders were prepared by the pyrolysis of triethylsilane ($(C_2H_5)_3SiH$; Kantoh Chemical, Tokyo, Japan) and trimethyl aluminum ($(CH_3)_3Al$; Nippon Aluminum Alkyls, Ltd., Tokyo, Japan), respectively, at 1100 °C. In order to eliminate any residual carbon, the SiC powder was further heated at 500 °C for 2 h in air; the Al_4C_3 powder was not similarly treated, due to its low oxidation resistance to form Al_2O_3.

For each specimen, 5 mol% of Al_4C_3 powder was added to the SiC powder and mixed in the presence of *n*-hexane using an alumina mortar and pestle. Following this, 0–50 mass% (0–47 vol%) of chopped Tyranno® Si–Al–C (SA) fiber (Ube Industries Ltd., Ube City, Japan) was added to the mixture; approximately 1.5 g of the resulting powder was uniaxially pressed at 50 MPa and then isostatically pressed at 100 MPa in order to form a disk of diameter 20 mm and thickness 1.5 mm. The compact was then hot-pressed at 1800 °C for 30 min in an Ar atmosphere under a uniaxial pressure of 31 MPa. The heating rate of the furnace was 30 °C min^{-1} from room temperature up to 1100 °C and then 10 °C min^{-1} from 1100 °C up to 1800 °C; the specimens were furnace cooled after the hot pressing procedure.

Evaluation

Crystalline phases of the powders and ceramic composites were identified using an X-ray diffractometer (XRD) (Model RINT2000PC, Rigaku, Tokyo). The relative density of the ceramic composite was calculated by dividing the bulk density by true density. The bulk density was measured on the basis of mass and dimensions, whereas the true density was measured picnometrically at 25 °C, using *n*-hexane as a replacement liquid after the specimen had been pulverized using an alumina mortar and pestle.

Flexural strength and fracture toughness measurements were carried out on rectangular specimens of dimensions 15 × 3 × 1.5 mm^3 cut from the hot-pressed compacts using a diamond saw and then polished to a 1 μm surface finish. For both cases the specimens were cut so that the load was applied parallel to the direction of hot pressing. The flexural strength measurement was conducted using the three-point bend configuration on a universal testing machine (Model YZ500-PC, Yasuda Precision Instruments, Tokyo) with a crosshead speed of 0.5 mm min^{-1} and a span of 10 mm. The flexural strength was calculated from the average of five specimens. Fracture toughness, K_{IC}, was determined using the single-edge notched beam (SENB) technique for specimens containing a notch (depth 1 mm and width 0.3 mm) introduced using a diamond saw. A span and cross-head speed of 10 mm and 0.5 mm min^{-1} were utilized, respectively, with each K_{IC} value being calculated from the average of five specimens.

It should be noted that whilst the saw blade thickness was nominally 0.3 mm, microscopy investigations indicated the notch tip radius to be 0.1 mm (100 μm) with the ''true'' notch radius being smaller and related to the size of the diamond saw grit [16]. For the present case, the notch radius due to machining-induced damage from the diamond saw grit was estimated to be on the order of 10 μm. It is known that the accurate determination of fracture toughness is dependent on several factors [16–19], particularly notch radius which should be no larger than the scale of the relevant microstructural or machining-induced defects. The grain size of the SiC matrix was typically submicrometer-scale; the fiber diameters and pore dimensions were similar to the dimensions of expected machining-induced damage, whilst the fiber lengths were at least an order of

magnitude larger. Thus, the likely scale of microstructure-limiting features (e.g., fiber dimensions) in the present composite would be significantly larger, compared to that found in fine-grained monolithic ceramics, i.e., larger notch radii would be allowed in the chopped fiber composite. The authors consequently considered the notch radius utilized in the present work to be appropriate for the chopped fiber composite under investigation.

Specimen fracture surfaces were investigated using a field emission scanning electron microscope (SEM) (Model S-4500, Hitachi, Tokyo; acceleration voltage, 5 kV) after the specimen surface had been coated with Pt–Pd using an ion coater (Model E-1030, Hitachi, Tokyo) in order to avoid charging effects.

Results and discussion

Properties of the component materials

The specific surface areas (SSA) of the starting SiC and Al_4C_3 powders were determined to be 53.4 and 58.0 $m^2\ g^{-1}$, respectively, with primary particle sizes (calculated on the basis of SSA and density) of 42 nm (SiC) and 39 nm (Al_4C_3). The XRD results (not presented here) indicated the SiC powder to be essentially amorphous, whereas the Al_4C_3 powder was composed of a single Al_4C_3 phase. Ultrafine SiC powder was utilized in the present work in order to minimize the hot pressing temperature and thus reduce any potential thermal degradation of the SA fiber, which is known to occur above 1900 °C [14]. Previous work by the authors had demonstrated the present mixture of SiC and Al_4C_3 powders to have been successfully densified at 1800 °C [10].

XRD patterns for the fibers indicated the presence of β-SiC, with the (111) and (220) reflections being unusually intense, i.e., the presence of anisotropic β-SiC crystals, together with a small amount of α-SiC, whilst the chemical composition obtained from the manufacturer's data was: Si, 67.8 mass%; Al, ≤ 2 mass%; C, 31.3 mass%; and O, 0.3 mass%.

The influence of mean fiber length on composite properties was investigated using three batches of SA fiber with fiber length distributions for each batch being checked using SEM. The results are shown in Fig. 1. The fiber lengths for the three batches were distributed in the ranges of 133–333 μm (mean: 214 μm), 200–600 μm (mean: 394 μm), and 350–1150 μm (mean: 706 μm), respectively; the fiber batches are referred to as SA(214), SA(394), and SA(706), respectively.

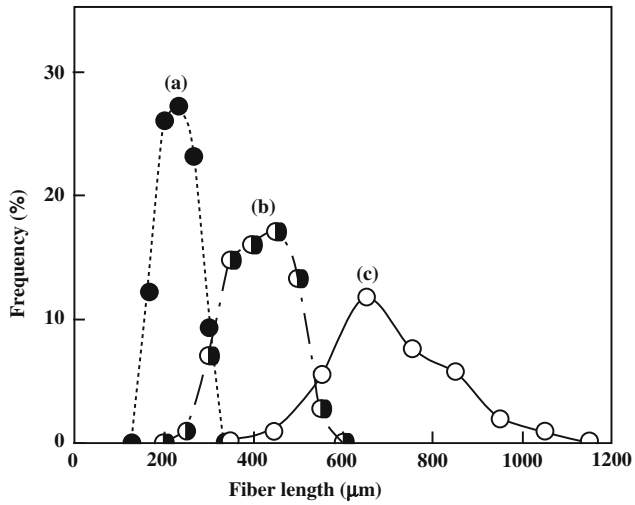

Fig. 1 Fiber length distributions for the Tyranno® Si–Al–C (SA) fibers with the mean length of (**a**) 214 μm, (**b**) 394 μm, and (**c**) 706 μm

Densification of SiC/SiC composites containing SA(706) fiber

The densification process of the SiC/SiC composites containing SA fiber was examined using the SA(706) fiber. The influence of fiber amount on relative density is shown in Fig. 2. Whilst the relative density of the monolithic SiC ceramic was 98.1 %, this decreased to 96.8% for the case of 20 mass% of SA(706) fiber addition and then increased to reach a maximum value of 98.5% for the case of 30 mass% fiber addition, i.e., the relative densities of the SiC composite specimens always exceeded 95%.

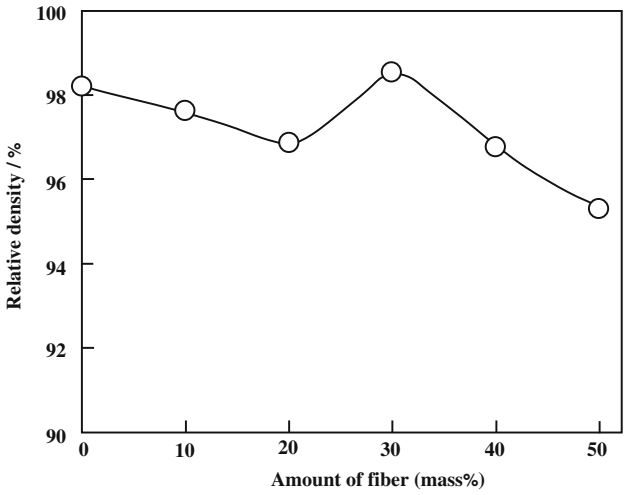

Fig. 2 Effect of SA(706) fiber addition on the relative density of SiC/SiC composites hot-pressed at 1800 °C for 30 min

In order to examine the alignment of SA(706) fibers within the composite specimens, microstructures of the SiC/SiC composites were observed using SEM. Typical SEM micrographs are shown in Fig. 3. It is apparent from the micrographs that most of the chopped SA(706) fibers were arranged perpendicular to the hot-pressing direction. This alignment is attributed to the initial uniaxial compaction of the powder mixture, together with the effect of the continuous uniaxial pressure during hot pressing. A similar alignment of fibers, i.e., perpendicular to the hot-pressing direction, has previously been observed by the authors in SiC/SiC composites containing chopped SZ fiber [10].

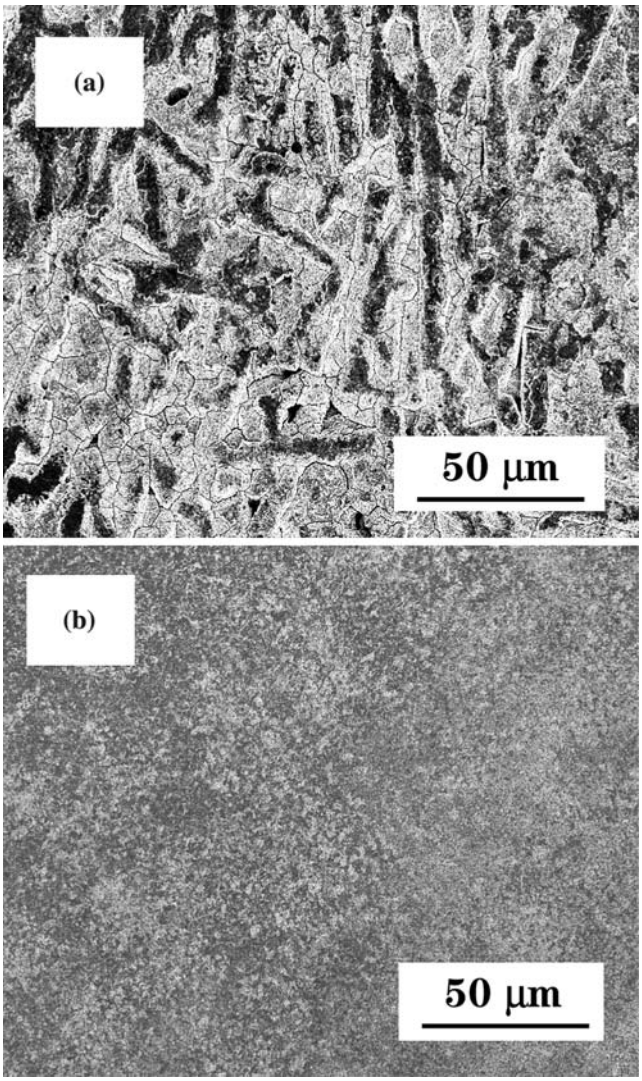

Fig. 3 SEM micrographs of the (**a**) surface and (**b**) cross section of the SiC/SiC composite containing SA(706) fiber addition hot-pressed at 1800 °C for 30 min. Note that the surface is located perpendicular to the hot-pressing direction, whereas the cross section is located parallel to the hot-pressing direction

The crystalline phases of the SiC/SiC composites containing SA(706) fiber were examined using XRD. Whilst not shown here, the presence of β-SiC and α-SiC, together with a small amount of Al_2O_3, was noted for all composites; moreover, no appreciable changes in XRD patterns were noted for the different fiber amounts. The presence of Al_2O_3 is attributed to the dehydration of a thin $Al(OH)_3$ layer often present on Al_4C_3 particles as a result of atmospheric moisture [20] and/or the solid-state reaction of Al_4C_3 with SiO_2 often present as a thin layer on the surfaces of SiC particles [21, 22].

According to the phase diagram of the Al–C system [23], the liquid phase may form when the temperature exceeds 1400 °C. It is, therefore, reasonable to assume that the liquid phase within the Al–C system is formed through the thermal decomposition of Al_4C_3. In addition, the liquid phase in the mullite ($3Al_2O_3{\cdot}2SiO_2$)-SiO_2 system may be formed (e.g., eutectic liquid at 1587 ± 10 °C [24]) during hot pressing. As is the case for many ceramic systems, the liquid phase formed during hot pressing would contribute to optimization of grain rearrangement, thereby leading to increased densification.

Mechanical properties of SiC/SiC composites containing SA(706) fiber

Following the fabrication of dense SiC/SiC composites containing SA(706) fiber addition, the flexural strength and fracture toughness were examined as a function of fiber amount. The results are shown in Fig. 4. Whereas the flexural strength of the monolithic SiC specimen was 293 MPa, this increased to a maximum of 344 MPa for 30 mass% of SA(706) fiber addition; however, it decreased to approximately 250 MPa with increasing fiber amount. The maximum value of 344 MPa was approximately 30% higher compared to that of previous researchers [13]. One interesting aspect of Fig. 4 may be that the trend in flexural strength closely followed that of relative density (Fig. 2), suggesting the flexural strength of this composite to be limited by the amount of residual porosity. The rationale behind this hypothesis may be that larger pores, generally formed by the coalescence of smaller pores at the latter stage of sintering, often lower the initial microcracking stress in the matrix. Thus the composite would fail either at, or close to, the stress required for initial microcracking, which indicates the toughening effect of the fibers to be minor in comparison with the case of continuous fiber-reinforced CMCs.

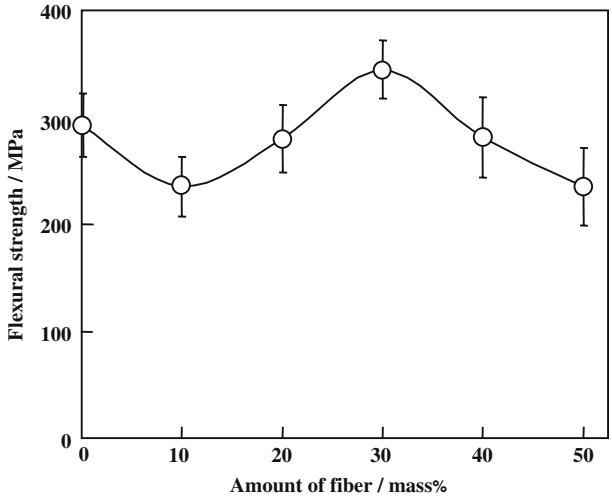

Fig. 4 Effect of SA(706) fiber addition on the flexural strength of SiC/SiC composites hot-pressed at 1800 °C for 30 min

Further evidence for this hypothesis is the linear nature of the stress–strain curves prior to failure.

The effect of SA(706) fiber addition on the composite fracture toughness is presented in Fig. 5. Whereas the fracture toughness of the monolithic SiC specimen was 2.8 MPa $m^{1/2}$, this increased with increasing fiber amount to reach a maximum of 4.7 MPa $m^{1/2}$ for 40 mass% of fiber addition. Further increases in fiber addition, however, decreased the fracture toughness down to 3.15 MPa $m^{1/2}$. Whilst these values are somewhat lower than those of continuous fiber-reinforced CMCs [4, 25], the degree of toughening behavior noted in these specimens is consistent with that reported for other discontinuous fiber-reinforced CMC systems [10].

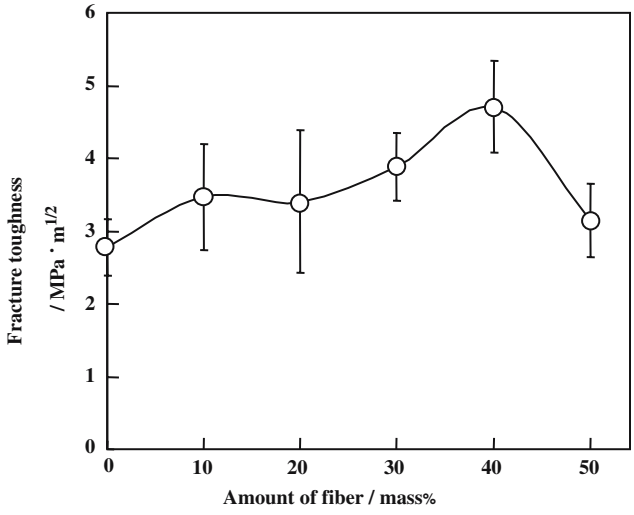

Fig. 5 Effect of SA(706) fiber addition on the fracture toughness of SiC/SiC composites hot-pressed at 1800 °C for 30 min

In order to clarify the fracture toughness behavior, fracture surfaces of SiC/SiC composites containing SA(706) fiber were investigated using SEM. Regardless of the increase in fracture toughness, no significant pullout of fibers was observed in any of the specimens. Only a limited degree of fiber debonding and porosity between individual fibers may have contributed to the increased fracture toughness. Whilst models exist for the mechanical behavior of discontinuous fiber reinforced CMCs [26, 27], the lack of experimental data makes further analysis of the present data difficult. However, the SEM analysis, when combined with the fracture toughness, flexural strength, and relative density data, appears to confirm that the present SiC/SiC composites failed either at, or shortly following, the onset of matrix microcracking. It is thus clear that potential exists for the further optimization of fracture toughness behavior within this system.

Effect of fiber length on the mechanical properties of SiC/SiC composites containing SA fiber

Thus far, the fabrication conditions required for the production of dense SiC/SiC composites containing SA(706) fiber have been clarified. In this section, the effect of SA fiber length on relative density and mechanical properties was further examined. The relative density and flexural strength of SiC/SiC composites containing 40 mass% of SA fiber are shown in Fig. 6, as a function of mean fiber length. Whereas the relative densities of the specimens always exceeded 96%, the flexural strength decreased from 380 to 281 MPa with increasing mean fiber length from 214 to 706 μm. The maximum value achieved, i.e., 380 MPa, was significantly higher compared to that obtained from similar SiC/SiC composites [13].

The effect of mean fiber length on fracture toughness is shown in Fig. 7. The fracture toughness increased almost linearly with mean fiber length, i.e., a value of 3.4 MPa $m^{1/2}$ being achieved for the composite containing SA(214) fiber and a maximum of 4.7 MPa $m^{1/2}$ for the case of SA(706) fiber. It is thus clear, as might be expected, that mean fiber length, i.e., aspect ratio, is an important factor in the toughening behavior of discontinuous fiber-reinforced CMCs [27]. It is, therefore, recommended that future work should investigate the effect of longer mean fiber length on the fracture toughness of this composite in order to determine the upper limit for this toughening mechanism.

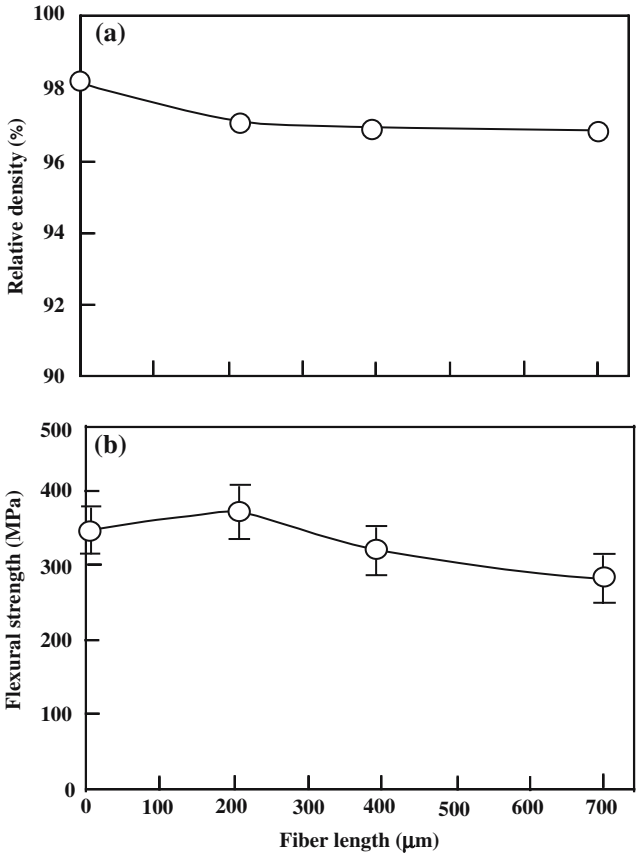

Fig. 6 Effect of SA fiber length on the (**a**) relative density and (**b**) flexural strength of SiC/SiC composites containing 40 mass% of SA fiber addition hot-pressed at 1800 °C for 30 min

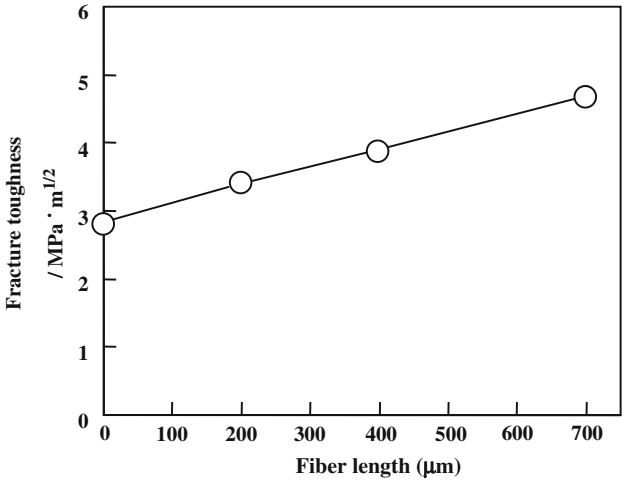

Fig. 7 Effect of SA fiber length on the fracture toughness of SiC/SiC composites containing 40 mass% of fiber addition hot-pressed at 1800 °C for 30 min

Effect of SA fiber with carbon interface on the fracture toughness of SiC/SiC composites

As shown earlier the fracture toughness of the SiC/SiC composite containing 40 mass% of SA(706) fiber (4.7 MPa $m^{1/2}$) was approximately 70% higher compared to that of the monolithic case (2.8 MPa $m^{1/2}$). Furthermore, one method commonly used to enhance the fracture toughness of CMCs is the utilization of a weakly bonding layered material, such as pyrolytic carbon (py-C) [28] or hexagonal boron nitride (h-BN) [29], at the fiber/matrix interface in order to promote crack deflection and fiber pullout [30]. Therefore, an additional batch of chopped SA fiber was used in this paper. This fiber had been surface-treated by the manufacturer by heating the standard SA fiber at 1700 °C for 1 h in a carbon monoxide atmosphere with the intention of producing a layer of py-C at the fiber interface. Typical SEM micrographs are shown in Fig. 8. Whereas the surface of the standard fiber, i.e., no carbon interface, was smooth, that of the

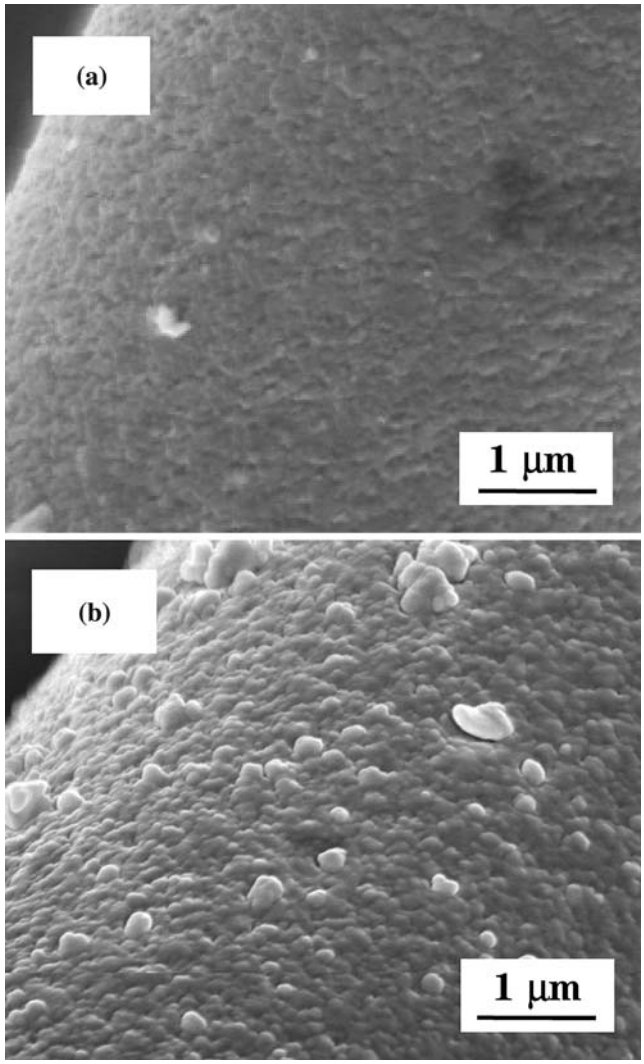

Fig. 8 SEM micrographs of the chopped SA fiber (**a**) without and (**b**) with a carbon interface.

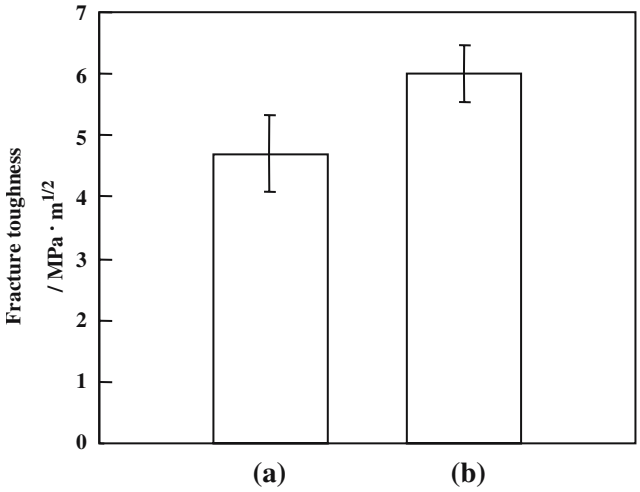

Fig. 9 Typical fracture toughness values of SiC/SiC composites containing 40 mass% of (**a**) SA(706) fiber addition and (**b**) SA(706)/C fiber addition hot-pressed at 1800 °C for 30 min

surface-modified fiber was relatively rough in nature [15]. According to Auger depth profiles provided by Ube Industries Ltd., the carbon concentration of the surface-modified fiber was almost 100% at the surface and decreased with increasing depth to reach a constant value for depths of greater than 100 nm; the carbon interface thickness was, therefore, estimated to be 100 nm.

In light of this, SiC/SiC composites containing 40 mass% of SA(706) fiber with a carbon interface (named ''SA(706)/C'') were fabricated using the same conditions as before. Typical fracture toughness values of SA(706) and SA(706)/C are shown in Fig. 9. Whereas the fracture toughness of the SiC/SiC composite containing 40 mass% of SA(706) fiber was shown to be 4.7 MPa $m^{1/2}$ (Fig. 9a), the use of SA(706)/C fibers increased this value to 6.0 MPa $m^{1/2}$ (Fig. 9b). To the authors' knowledge, this value is believed to be the highest so far achieved for this type of chopped fiber-reinforced SiC/SiC composite. The main result of this work is that the fracture toughness of the SiC/SiC composite containing SA(706)/C fiber was more than double that of the monolithic case. The high fracture toughness may be attributed to the carbon layer at the fiber surface. In spite of this further improvement in fracture toughness behavior, however, SEM micrographs for this composite still revealed the lack of any distinct pullout phenomenon and, therefore, there most likely exists the potential for further increases in the fracture toughness, e.g., through the use of larger mean lengths.

Conclusion

The conditions required for the fabrication of dense silicon carbide (SiC) composites containing chopped Tyranno® Si–Al–C (SA) fiber, together with the mechanical properties (flexural strength and fracture toughness) of the resulting composites were investigated for SiC/SiC composites containing 0–50 mass% of SA fiber (mean length: 214 μm (SA(214)), 394 μm (SA(394)), and 706 μm (SA(706)) manufactured using the hot-pressing technique at 1800 °C for 30 min under a uniaxial pressure of 31 MPa. The results obtained are summarized as follows:

(1) The relative densities for all SiC/SiC composites containing SA(706) fiber exceeded 96% with maximum values of flexural strength (344 MPa) and fracture toughness (4.7 MPa $m^{1/2}$) being achieved for 30 mass% and 40 mass% of SA(706) fiber, respectively. Increasing the mean fiber length from 214 to 706 μm indicated the flexural strength to decrease from 380 to 281 MPa for 30 mass% of fiber, whereas the fracture toughness increased from 3.4 to 4.7 MPa $m^{1/2}$ for 40 mass% of fiber.

(2) SA(706) fibers containing an approximately 100 nm surface layer of carbon (SA(706)/C) were also used as a reinforcement for the composite. The fracture toughness of the composite containing 40 mass% of SA(706)/C fiber was 6.0 MPa $m^{1/2}$, which is more than double that of the monolithic case.

Acknowledgements The authors wish to express their thanks to Dr. M. Shibuya of Ube Industries, Ltd., for providing the Tyranno® Si–Al–C fibers used in this work and for measuring the Auger depth profile of the SA(706)/C fiber.

References

1. Srinivasan M, (1989) Treatise on materials science and technology, vol 29. Academic Press, Inc., p 99
2. Schlichting J, Riley FL (1991) In: Brook RJ (ed) Concise encyclopedia of advanced ceramic materials, Pergamon press, Oxford, UK, p 426
3. Pluvinage P, Parvizi-majidi A, Chou TW (1996) J Mater Sci 31:232
4. Ishikawa T, Yamamura Y, Hirokawa T, Hayashi Y, Noguchi Y, Matsushima M (1993) In: Miravette A (ed) Proceedings of the ninth international conference on composite materials, Woodhead publishing Co., Cambridge, UK, p 137
5. Dong SM, Chollon G, Labrugere C, Lahaye M, Guette A, Naslain R, Jiang DL (2001) J Mater Sci 36:2371
6. He M-Y, Hutchinson JW (1989) Int J Solids Structures 25:1053

7. Evans AG, He M-Y, Hutchinson JW (1989) J Am Ceram Soc 72:2300
8. Evans AG, Zok FW (1994) J Mater Sci 29:3857
9. Davies IJ, Abe S, Pezzotti G, Kleebe H-J, Nishida T (2000) Maters Letts 43:203
10. Itatani K, Hattori K, Harima D, Aizawa M, Okada I, Davies IJ, Suemasu H, Nozue A (2001) J Mater Sci 36:3679
11. Lee J-S, Yoshida K, Yano T (2002) J Ceram Soc Jpn 110:985
12. Lee J-S, Imai T, Yano T (2003) Maters Sci Eng A339:90
13. Lee J-S, Yano T (2004) J Eur Ceram Soc 24:25
14. Ishikawa T, Kohtoku Y, Kumagawa K, Yamamura T, Nagasawa T (1998) Nature 391:773
15. Itatani K, Tanaka T, Suemasu H, Nozue A, Davies IJ (2005) J Australasian Ceram Soc 41:1
16. Damani R, Gstrein R, Danzer R (1996) J Eur Ceram Soc 16:695
17. Nishida T, Hanaki Y, Pezzotti G (1994) J Am Ceram Soc 77:606
18. Rieder K-A, Tschegg EK, Harmuth H (1998) J Maters Sci Letts 17:675
19. Mukhopadhyay AK, Datta SK, Chakraborty D (1999) Ceramics Int 25:447
20. Suemitsu T, Takashima A, Nishikawa H (1995) J Am Ceram Soc 103:479
21. Powers JM, Somorjai GA (1991) Surf Sci 244:39
22. Zhang Y, Binner J (2002) J Am Ceram Soc 85:529
23. Okamoto H (1992) J Phase Equil 13:97
24. Pask JA, Aksay IA (1975) J Am Ceram Soc 58:507
25. Kim Y-W, Lee J-G, Kim M-S, Park J-H (1996) J Mater Sci 31:335
26. Akatsu T, Tanabe Y, Yasuda E (1999) J Mater Res 14:1316
27. Suemasu H, Kondo A, Itatani K, Nozue A (2001) Compos Sci Technol 61:281
28. Kmetz M, Suib S, Galasso F (1990) J Am Ceram Soc 73:3091
29. Prouhet S, Camus G, Lamrugere C, Guette A, Martin E (1994) J Am Ceram Soc 77:649
30. Thouless MD, Sbaizero O, Sigl LS, Evans AG (1989) J Am Ceram Soc 72:525